*Journal of Nepal Geological Society, 2006, Vol. 34, pp. 39–46*

# Critical stress level causing rock failure: a case study of Melamchi tunnel from central Nepal Himalaya

***G. L. Shrestha and E. Broch**
*Department of Geology and Mineral Resources Engineering,*
*Norwegian University of Science and Technology, Trondheim 7491, Norway*
*(*Email: gyanendra.shrestha@geo.ntnu.no)*

## ABSTRACT

The determination of critical stress level is important in tunnel stability assessment. In this paper, the results of laboratory test on rock samples from the proposed Melamchi tunnel alignment in central Nepal are presented. In order to determine the critical stress level, creep tests were carried out on the gneissic rock cores. Time-dependent deformation curves were used to estimate the steady-state deformation rate for a given constant stress level.

The creep test curves were fitted with Burger's model and the rheological parameters were calibrated as suggested by previous researchers. Tunnel deformations were calculated for various time periods at a given stress level. On the basis of the creep test results at various uniaxial stress levels at constant temperature, an equation is given for the relationship between the strain rate and stress level.

## INTRODUCTION

One of the factors that may cause stability problems in tunnels is the stress level acting around underground openings. It is evident that a tunnel fails when the stress exceeds the strength of rock mass around the opening. If the stress level does not exceed the rock mass strength, but is sufficient to cause creep, it may lead to rock failure after some time. If the creep remains below the critical stress level, it does not lead to rock failure. Excavation causes changes in stress system around an opening. The effect of changed stress conditions is reflected in ground response which subsequently influences support pressure and may even lead to tunnel closure. Hence the prediction of ground response indicating the failure strength of the rock mass is very important for cost-effective and trouble-free tunnel construction.

Even if the concentrated stress level around a tunnel is below the rock mass strength, it still may cause creep. The 'critical stress level' is the minimum stress level which causes rock failure by creep after certain time. Aydan et al. (1993) considered the concept of analogy between the axial stress–strain response of rocks in laboratory tests and tangential stress–strain response of rocks surrounding the openings in tunnels. For a circular tunnel in homogeneous and isotropic rock under hydrostatic pressure ($\sigma_0$) and without (or with support pressure $<\sigma_0$) support application, tangential stress $\sigma_\theta$ acts as the major principal stress $\sigma_1$ and radial stress $\sigma_r$ acts as the minor principal stress $\sigma_3$. At the tunnel contour, $\sigma_r$ is zero and hence $\sigma_3$ indicates the required tunnel support pressure $p_i$ (Duncan-Fama 1993; Aydan et al. 1993).

A complete stress–strain curve can also be used to predict rock failure as a result of constant stress. As shown in Fig. 1, the locus of a creep test in stress–strain graph is a horizontal line. If the initial stress in the rock is close to the peak load, any creep will terminate in rupture when the accumulated strain intersects the falling part of the complete stress–strain curve. A creep test started at the point A will terminate in a rupture at the point B in a relatively short time.

A creep test began at C will terminate in a rupture at D after a much longer time. And a creep test initiated at E below the critical stress level G will approach point F and stop at a finite strain without rupture after a long time. Below T (creep threshold) there is no creep. If a number of creep tests are performed, each one for a different value of the applied stress (between levels T and U), the results obtained can be plotted by giving the terminal locus of the long-term creep test (TU). The line TU is the terminal locus of long-term creep tests. Above level U (or G), the minimum creep rate (secondary) increases with the stress level and the test terminates with tertiary creep and fracture when the accumulated strain has reached a finite value, given by the descending part of the curve.

This shows that a rock mass may creep to failure even if it has not failed immediately after the excavation. Failure takes place as the creep line intersects the falling part of the stress–strain curve.

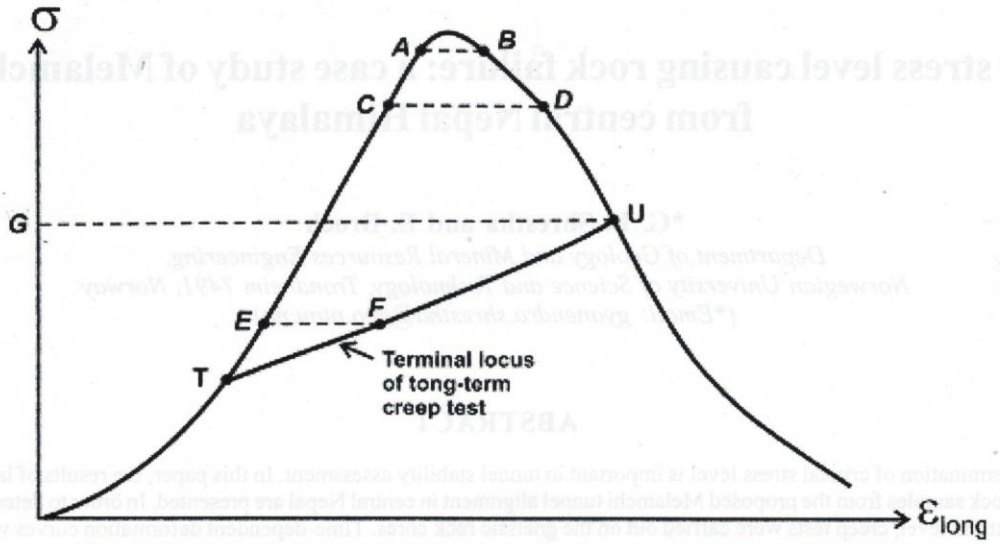


**Fig. 1: Creep in relation to the complete stress–strain curve (Goodman 1989)**

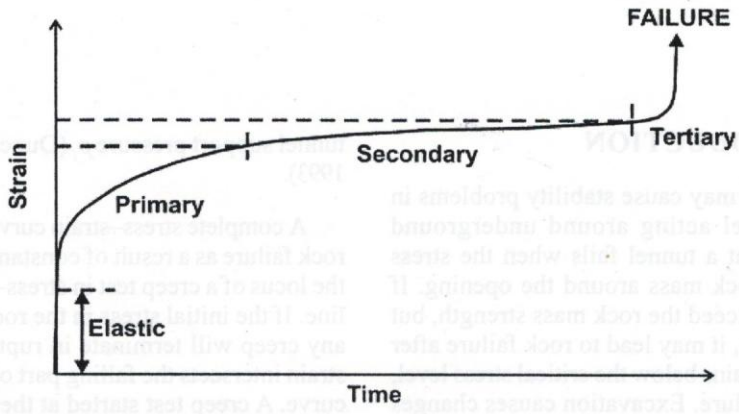


**Fig. 2: Regions of behaviour in creep (University of Saskatchewa 2003)**

The time-dependent deformation (creep) caused tunnel sidewall spalling in the 'Clarens' sandstone in Lesotho having a uniaxial compressive strength (UCS) to vertical stress ratio as high as 4 (Broch 1996), whereas overstressing always occurred where the ratio was lower than 2.5. These phenomena were observed several weeks after the excavation. These stress-induced spalling phenomena were rather different from the violent rockbursting, which is a normal case in Scandinavian hard crystalline rocks. Similarly, the deformation in a squeezing section of the Taw Tunnel in Japan continued for more than 1500 days after the completion of excavation (Aydan et al. 1996).

The strain–time curve for a creep test has a very characteristic form. Initially, as the load is applied, the elastic strain occurs virtually instantaneously. As time passes under the constant stress, the rate of strain decreases. The period of decelerating strain rate is called the primary creep. The primary creep phase is followed by an extended period of slow (almost steady-state) deformation called the secondary creep. At the end of this stage, the strain rate begins to accelerate and the material rapidly fails. The final stage of accelerating deformation is called the tertiary creep.

Creep in rock masses is associated with crack propagation. During the primary creep phase the rock 'acclimatises' to the stress and crack propagation slows to a stable, almost constant rate. During the 'steady' secondary creep stage, the material is damaged more and more until finally, in the tertiary stage, uncontrolled accelerating crack propagation leads to failure.

Thus determination of the critical stress level is useful for the assessment of tunnel stability. In this paper, laboratory tests and analysis were carried out for the Melamchi tunnel

situated in central Nepal Himalaya and the details are given in the following sections.

## MELAMCHI WATER SUPPLY PROJECT

The main objective of the Melamchi Water Supply Project (MWSP) is to provide an efficient and safe potable water supply which will result in improved health conditions and economic development in the Kathmandu valley.

This project consists of a 26.3 km long tunnel with 3 adits (i.e. at Ambathan, Gyalthum, and Sindhu) and intake structures. Its maximum tunnel overburden is about 1,200 m. The access will be provided to seven working areas along the tunnel alignment. The theoretical cross-sectional area of the tunnel is 12.7 $m^2$, except for adits and the tunnel section upstream of the Ambathan adit (with an area of 18.4 $m^2$). The tunnel gradient varies between 1.2 and 6%, except for the stretch between the Ambathan adit and intake where it is 44%.

### Geological investigations

The project area is located within the Precambrian Bhimphedi Group of the Kathmandu Complex. Geological formations along the tunnel have been assessed from the intake to outlet as (Norplan 2002):

- Timbu Formation: migmatite and banded gneiss with subordinate quartzite and schist, intensely deformed and folded (0 – 6.6 km of tunnel length)
- Bolde Quartzite: massive quartzite with sporadic schist bands ( 6.6 – 8.2 km of tunnel length)
- Gyalthum Formation: alternation of laminated quartzite and banded schist ( 8.2 – 19.5 km of tunnel length)
- Sheopuri Injection Gneiss zone: banded, augen, and granitic gneiss (19.5 – 26.3 km of tunnel length)

In the course of Melamchi project development, various types of investigations were carried out at different stages. Geological mapping and exploratory diamond core drilling were carried out during the first detailed study by Snowy Mountain Engineering Corps (SMEC). Similarly, geological mapping and seismic refraction study were done during the second detailed study by BPC Hydroconsult (BPC 1996).

During the third (present) detailed study exploratory diamond core drilling was carried out at the tunnel or adit portals and along the tunnel. A total of 33 holes were drilled with a total length of about 200 m. At the same time, rock mechanical testing of core samples in the laboratory and permeability (packer) testing were carried out in the exploratory holes. The average RQD values of the core samples from the Timbu Formation and Sheopuri Injection Gneiss zone were classified as Poor (25–50%) while those from the Gyalthum Formation were categorised as Very Poor (0 – 25%).

### Collection of samples for laboratory test

Among the four rock groups, the Gyalthum Formation has been considered to be the weakest one. Moreover, it is inferred that the rock has three weak zones and the maximum overburden above the tunnel alignment in this formation is about 550 m. Hence, this formation is expected to encounter squeezing problems. It would be ideal to carry out laboratory tests on the samples from this formation, but due to very poor (0–25%) RQD values of the drilled cores the test samples could not be obtained. The test samples were obtained from the Sheopuri Gneiss as it had the lowest uniaxial compressive strength of 30 MPa with good RQD values. The tunnel within this formation may suffer from squeezing problems as there is up to 850 m thick overburden.

A study on creep or long-term deformation of rock was carried out on ten samples (all of 33 mm in diameter) in the laboratory of the Department of Geology and Mineral Resources Engineering, the Norwegian University of Science and Technology, Norway. The specimens were collected from the borehole TDH1 driven in the Sheopuri Gneiss. It is one of the six boreholes drilled along the tunnel alignment (Table 1).

## CRITICAL STRESS LEVEL FOR CREEP FAILURE

The critical stress level was determined by long-term deformation (creep) tests at various axial stress levels. Sample No. 1 was tested in air-dry (room temperature) conditions whereas the remaining ones were saturated first and then all of them were subjected to a constant load until they failed.

The time-dependent strain responses for the six creep tests are presented in Fig. 3. All the samples, except one at

**Table 1: Some features of the exploratory hole TDH1 and cores from it**

| Location, chainage | Main tunnel alignment at Shivapuri, 25.250 km |
|---|---|
| Length, orientation | 150 m, vertical |
| Elevation, Co-ordinates | 1640 m, 641212 E, 3073435 N |
| Overburden thickness to bedrock | 10.3 m |
| Average RQD | 35 |
| Depth to ground water | 1.0 m |
| Average core loss | 21 % |
| Average Point load index $I_s(50)$ | Diametric 3.7, Axial 4.3 |
| Average UCS (MPa) | 30.0 |

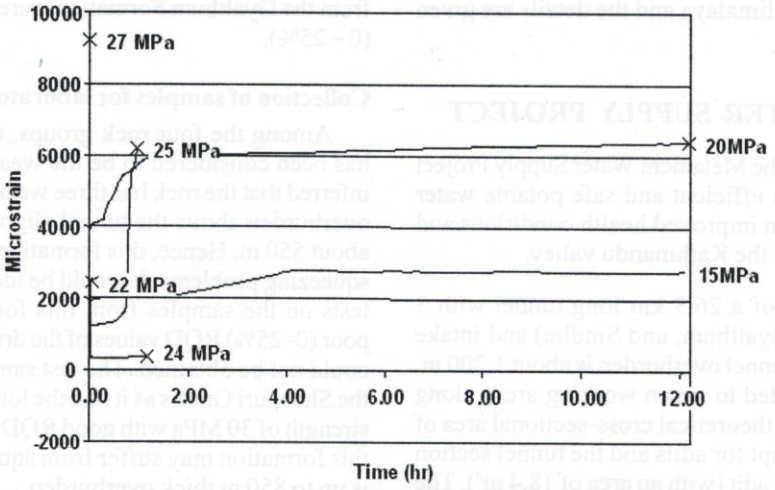


**Fig. 3: Strain–time curves for creep on the Sheopuri Gneiss at different stress levels**

**Table 2: The applied stress levels and the corresponding failure time in the creep tests on the Sheopuri Injection Gneiss from borehole TDH1**

| Sample No. | Length (mm) | Stress applied (MPa) | Time taken to failure |
|---|---|---|---|
| 2-4 | 82 | 27 | 25 seconds |
| 4-2 | 81 | 25 | 1 hour |
| 4-4 | 83 | 24 | 1 hour 10 minutes |
| 1 | 81 | 25 (already used in cyclic loading) | 1 minute |
| 412 | 79 | 20 | 12 hours |
| 41 | 79 | 19.2 (load applied at once) | 7 seconds |
| 42 | 82.2 | 22 | 4 minutes |
| 43 | 82 | 15 –16 | did not break |
| 45 | 82 | 15 – 16 | did not break |
| 410 | 79.5 | 20.5 (already used in progressive creep) | 3 minutes |

16 MPa stress level, failed after a certain period of time. The symbol 'x' at the end of the curve indicates the sample failed at the end of the creep test.

Sample 412 failed in 12 hours after it was subjected to a constant stress level of 20 MPa. It is the lowest stress level that caused the creep failure. An average uniaxial compressive strength (UCS) of these samples was 39 MPa. According to the test results, samples subjected to 50% or higher UCS of intact rock samples failed by creep. Thus the critical stress level for creep failure for the Sheopuri Gneiss is 20 MPa.

In ideal conditions, the time to failure should decrease with the increase of stress level applied for the creep test. This trend is maintained in the test results given in Fig. 3

**Table 3: Rheological parameters from creep test at different stress levels**

| Sample | Stress level (MPa) | Shear modulus, $G_1$ (Pa) | Shear modulus, $G_2$ (Pa) | Viscosity, $\eta_1$ (Pa-hr) | Viscosity, $\eta_2$ (Pa-hr) |
|---|---|---|---|---|---|
| 45 | 15 | $5.4054*10^9$ | $3.027*10^9$ | $6.3593*10^9$ | $2.2425*10^{12}$ |
| 412 | 20 | $2.666*10^9$ | $2.087*10^9$ | $8.333*10^8$ | $1.6648*10^{11}$ |
| 4-2 | 25 | $1.282*10^{10}$ | $2.961*10^{10}$ | $1.068*10^8$ | $3.754*10^{10}$ |

except for the case of 22 MPa stress level. Two possible reasons for it are: (1) the samples are heterogeneous and the heterogeneity varies from one sample to another and (2) there was no control on the loading rate, which might have caused some impact on the sample.

## TIME-DEPENDENT TUNNEL DEFORMATION

The time-dependent tunnel deformation is calculated using the rheological parameters of the rock. These parameters have been quantified by calibrating the strain–time curve obtained from the creep tests. The calibration is carried out for the Burger substance in axial loading conditions. Out of the six curves in Fig. 3, only three representative strain–time curves, namely those for 15, 20, and 25 MPa stress levels, have been calibrated. The stress level and the respective calibrated rheological parameter values are given in Table 3.

The rheological parameters given in Table 3 correspond to the intact rock condition loaded under constant stress level at 20 ÚC and with a humidity range of 65–70 %. Here, a circular tunnel with a hydrostatic stress has been considered and the support is assumed to act uniformly on the entire perimeter of the tunnel of 2.5 m radius.

**Table 4: Total radial deformation (mm) calculated for Melamchi tunnel at three different tangential stress levels for 24 hours**

| Time (hr) | Tangential stress 25 MPa | Tangential stress 20 MPa | Tangential stress 15 MPa |
|---|---|---|---|
| 0.00 | 0.53 | 5.99 | 3.10 |
| 0.25 | 1.85 | 8.59 | 3.43 |
| 0.50 | 1.95 | 9.77 | 3.70 |
| 0.75 | 2.06 | 10.31 | 3.92 |
| 1 | 2.16 | 10.56 | 4.09 |
| 2 | 2.58 | 10.82 | 4.52 |
| 3 | 3.00 | 10.90 | 4.71 |
| 4 | 3.41 | 10.98 | 4.79 |
| 3 | 3.83 | 11.05 | 4.83 |
| 6 | 4.24 | 11.13 | 4.85 |
| 7 | 4.66 | 11.20 | 4.86 |
| 8 | 5.08 | 11.28 | 4.86 |
| 9 | 5.49 | 11.35 | 4.87 |
| 10 | 5.91 | 11.43 | 4.87 |
| 11 | 6.33 | 11.50 | 4.88 |
| 12 | 6.74 | 11.58 | 4.88 |
| 13 | 7.16 | 11.65 | 4.89 |
| 14 | 7.57 | 11.73 | 4.89 |
| 15 | 7.99 | 11.80 | 4.89 |
| 16 | 8.41 | 11.88 | 4.90 |
| 17 | 8.82 | 11.95 | 4.90 |
| 18 | 9.24 | 12.03 | 4.91 |
| 24 | 11.74 | 12.48 | 4.93 |

The following equation has been used to calculate deformations for an unsupported tunnel.

$$u_r(t) = \frac{\sigma_0 R}{2G_2} + \frac{\sigma_0 R}{2G_1} - \frac{\sigma_0 R}{2G_1} e^{-(G_1 t/\eta_1)} + \frac{\sigma_0 R}{2\eta_2} t \quad (1)$$

The constant stress in the creep test corresponds to the tangential stress level in the tunnel. For the sake of simplicity the tangential stress $\sigma_\theta$ is considered to be double of the overburden pressure. Hence a tangential stress of 15, 20, and 25 MPa correspond to the hydrostatic stress $\sigma_0$ of 7.5, 10, and 12.5 MPa respectively. Calculations were carried out for the total deformation including the instantaneous and time-dependent ones. In the above equation, the first part on the right-hand side gives the instantaneous deformation and the rest 3 parts give the time-dependent deformation. The total radial deformations calculated for the Melamchi tunnel at different tangential stresses are given in Table 4.

Fig. 4 shows the response of the total deformation with time. It can be observed that with the increase of the stress

**Table 5: Creep test data for calculating effect of stress level on the steady-state creep rate**

| Sample | Stress (Pa) | $Log_{10}$ stress (Pa) | Steady-state creep rates | $Log_{10}$ creep rates (1/s) |
|---|---|---|---|---|
| 45 | 1.5 E+07 | 7.176 | 1.7 E-06 | -5.769 |
| 412 | 2.0 E+07 | 7.301 | 40 E-06 | -4.398 |
| 4-2 | 2.5 E+07 | 7.398 | 800 E-06 | -3.097 |

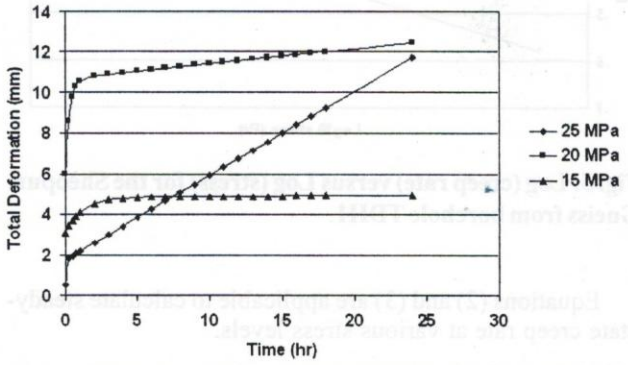


**Fig. 4: Comparison of time-dependent deformations for three different tangential stress levels in the Melamchi tunnel**

level, the deformation rate also increases, being 0.004, 0.08, and 0.41 mm/hr for 15, 20, and 25 MPa tangential stress levels respectively. A similar trend also applies to the case of instantaneous deformation. These amounts have been found to be 3.1 and 5.99 mm for 15 and 20 MPa stress levels respectively. However, it was only 0.53 mm in case of the 25 MPa tangential stress level, whereas it was supposed to be more than 5.99 mm. This discrepancy might have been caused by the rock anisotropy varying from one sample to another and uncontrolled loading rate.

## STEADY-STATE DEFORMATION RATE

For soft rocks the steady-state creep rate depends on the stress level (Lama and Vukuturi 1978). It is also true for hard and strong rocks (Malan 1998). The steady-state creep rate is almost constant at a given stress level for the gneissic rock samples from the borehole TDH1. Thus this rate multiplied by time gives the steady-state deformation for a given time period. The total deformation for a given time period can be estimated by adding instant and steady-state deformations together. However, it will underestimate the total deformation as it does not include the primary-state creep deformation.

The steady-state strain rate ($\dot{\varepsilon}_{ss}$) itself is a useful piece of information. It helps in predicting tunnel convergence rate. On the basis of creep test results, an equation can be established for calculating the stress ($\sigma$) dependent steady-state strain rate. The necessary creep test results for the calculation are given in the Table 5. The test results show that higher stress levels lead to higher creep rates.

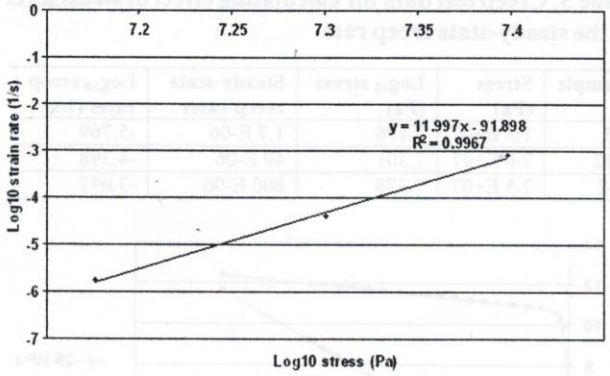


**Fig. 5: Log (creep rate) versus Log (stress) for the Sheopuri Gneiss from borehole TDH1**

Equations (2) and (3) are applicable to calculate steady-state creep rate at various stress levels.

$$\dot{\varepsilon}_{ss} = A'\sigma^{n} \quad (2)$$

$$\log \dot{\varepsilon}_{ss} = \log A' + n \log \sigma \quad (3)$$

Fig. 5 shows the plot of $log\, \dot{\varepsilon}_{ss}$ versus $log\, \sigma$. The values of log $A'$ and n are given respectively by the intercept and slope of the line in Fig. 5.

Fig. 5 gives values of 11.997 for n and -91.898 for $log_{10} A'$. Accordingly it assigns a value of 1.2647E-92 to A'. Replacing the values of $n$ and $A'$ in Equation (2), it gives

$$\dot{\varepsilon}_{ss} = 1.265 * 10^{-92} \sigma^{12} \quad (4)$$

Using Equation (4), the steady-state strain rate can be estimated for any constant stress level for the rock samples from the borehole TDH1.

## NUMERICAL MODELLING

FLAC $^{3D}$ code was used to simulate and analyse the stability of the unlined tunnel in the Sheopuri Gneiss. An inverted D-shaped tunnel was used for the present modelling purpose. The Time effect was incorporated in this modelling so that any time-dependent tunnel deformation could be assessed. Mohr model was used to simulate the tunnel excavation in the rock mass. It gives the tunnel deformation without considering the time-dependent effect. Then the time-dependent deformation was obtained using the Burger's model. The Burger's model needs rheological parameters. The stress level and the respective calibrated rheological parameter values are given in Table 3.

The required inputs are generated by laboratory tests on the samples obtained from the drilled rock cores. In order to determine the mechanical properties of rock materials, tests were carried out at the Sintef Laboratory of the Norwegian University of Science and Technology. Average values of all the test results given below are from the tests on saturated intact specimens (33-mm in diameter) from the borehole TDH1.

**Table 6: Input data for numerical modelling obtained using 'RocLab' for GSI = 45*.**

| Cohesion (MPa) | Friction angle (degree) | Tensile strength (MPa) | Deformation modulus (MPa) | Shear modulus (MPa) | Bulk modulus (MPa) |
|---|---|---|---|---|---|
| 2.33 | 36.2 | 0.027 | 4683 | 1935 | 2691 |

*From the RocLab Reference – considering the 'very blocky and fair' condition for jointed rock mass

UCS of intact rock $\sigma_{ci}$ =39 MPa, Elasticity modulus $E$ = 33.5 GPa, Poisson's ratio $\upsilon$ = 0.21, and density $\gamma$ = 0.027 MN/m$^3$.

Based on the laboratory tests, 'Roclab' software was used to generate other necessary parameters for the given rock mass condition (e.g. GSI = 45; see Table 6).

*Tunnel deformation with time effect*

Fig. 6 shows the tunnel deformation pattern for 24 hours. The instantaneous deformation was 8 mm and it continued to increase and exceeded 15 mm in 8 hours. Then the deformation did not alter. These results were obtained for the tunnel crown. The tunnel was found to be stable. Here the maximum principal stress in the tunnel crown and walls was 17.26 MPa. It caused the tunnel to deform for some time and then it stopped. As the critical stress level of 20 MPa was higher than the stress (17.26 MPa) acting on the tunnel crown and walls, the rock did not fail.

*Maximum principal stress*

Fig. 7 is a typical graphical presentation showing the location and magnitude of the maximum principal stress, which was the redistribution of the in situ stress after the tunnel excavation. It is to be noted that the in situ hydrostatic stress value was only 10 MPa but the stress value reached up to 17.26 MPa at the tunnel crown and the walls. The maximum principal stress is compressive as indicated by the negative signs in the legend of Fig. 7.

## DISCUSSIONS AND CONCLUSIONS

The critical stress level for the Sheopuri Gneiss from the borehole TDH1 was found to be 20 MPa. Thus the stress above the critical level may lead to failure even if it does not exceed the rock mass strength.

The strain–time curves were calibrated to obtain the rheological parameters. Based on these parameters, tunnel deformations were calculated by an analytical method for the three stress levels and also by numerical modelling for one stress level. Tunnel deformation (for 24 hours) by the analytical method and the numerical modelling at 20 MPa stress level, are 12.5 mm and 15 mm respectively. The

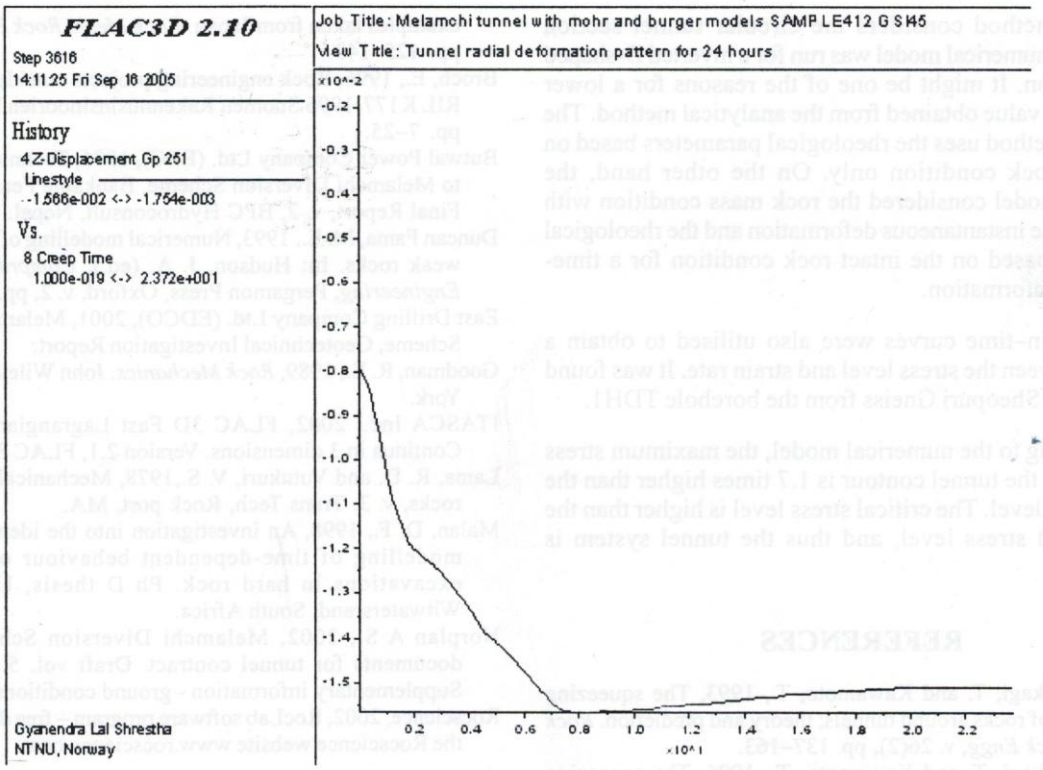


**Fig. 6: Tunnel crown deformation pattern for 24 hours**

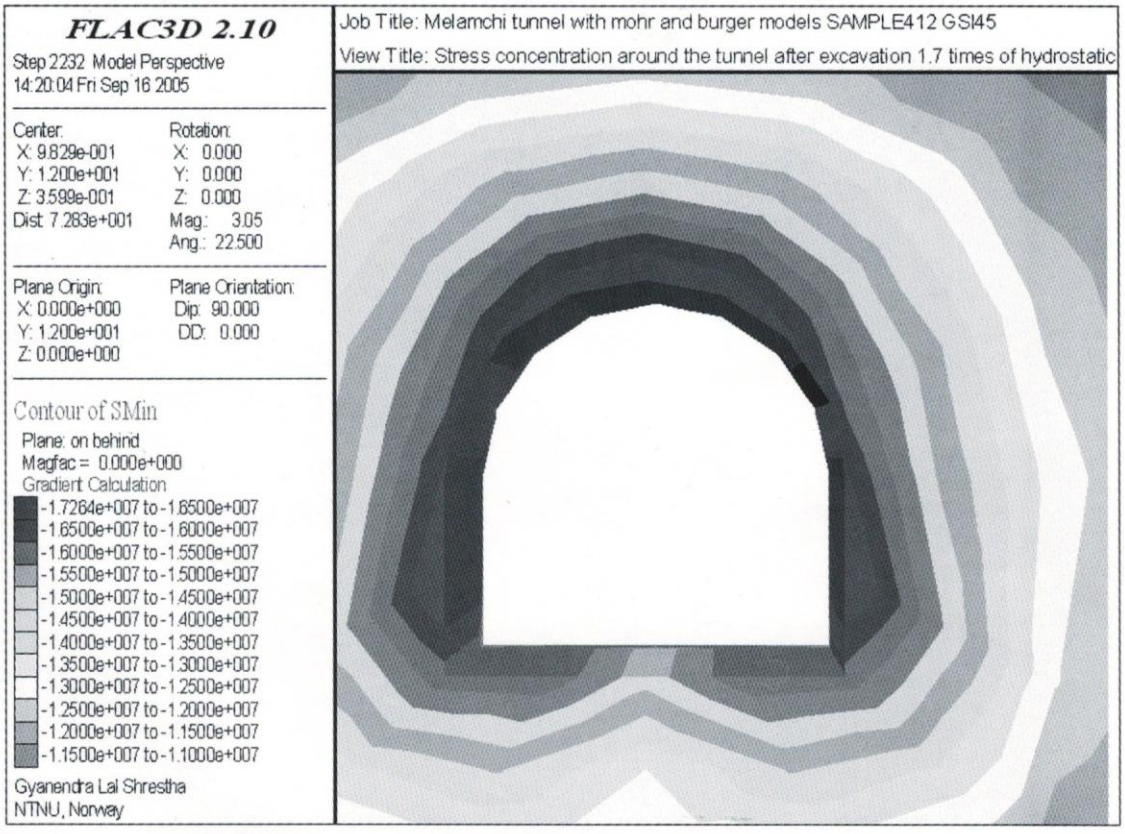


**Fig. 7: Location and magnitude of the maximum principal stress in rock mass after tunnel excavation**

analytical method considers the circular tunnel section whereas the numerical model was run for a inverted D-shaped tunnel section. It might be one of the reasons for a lower deformation value obtained from the analytical method. The analytical method uses the rheological parameters based on the intact rock condition only. On the other hand, the numerical model considered the rock mass condition with GSI 45 for the instantaneous deformation and the rheological parameters based on the intact rock condition for a time-dependent deformation.

The strain–time curves were also utilised to obtain a relation between the stress level and strain rate. It was found to be for the Sheopuri Gneiss from the borehole TDH1.

According to the numerical model, the maximum stress level around the tunnel contour is 1.7 times higher than the in situ stress level. The critical stress level is higher than the concentrated stress level, and thus the tunnel system is stable.

## REFERENCES


Aydan, O., Akagi, T. and Kawamoto, T., 1993, The squeezing potential of rocks around tunnels; theory and prediction. *Rock Mech. Rock Engg*, v. 26(2), pp. 137–163.

Aydan, O., Akagi, T. and Kawamoto, T., 1996, The squeezing potential of rock around tunnels: theory and prediction with examples taken from Japan. *Rock Mech. Rock Engg*, v. 29(3), pp. 125–143.

Broch, E., 1996, Rock engineering projects outside Scandinavia. RIL K177-1996 Suomen Rakennusinsinoorien Liitto RIL r. y. pp. 7–25.

Butwal Power Company Ltd. (BPC), 1996, Technical Assistance to Melamchi Diversion Scheme, Bankable Feasibility Study. Final Report, v. 2, BPC Hydroconsult, Nepal.

Duncan Fama, M. E., 1993, Numerical modelling of yield zones in weak rocks. In: Hudson, J. A. (ed.), *Comprehensive Rock Engineering*, Pergamon Press, Oxford, v. 2, pp. 49–75.

East Drilling Company Ltd. (EDCO), 2001, Melamchi Diversion Scheme, Geotechnical Investigation Report.

Goodman, R. E., 1989, *Rock Mechanics*. John Wiley & Sons, New York.

ITASCA Inc., 2002, FLAC 3D Fast Lagrangian Analysis of Continua in 3 dimensions. Version 2.1, FLAC 3D manual.

Lama, R. D. and Vutukuri, V. S.,1978, Mechanical properties of rocks, v. 3. Trans Tech, Rock port, MA.

Malan, D. F., 1998, An investigation into the identification and modelling of time-dependent behaviour of deep level excavations in hard rock. Ph D thesis, University of Witwatersrand, South Africa.

Norplan A S., 2002, Melamchi Diversion Scheme, Tender documents for tunnel contract. Draft vol. 5.1, section 11 Supplementary information - ground conditions.

Rocscience, 2002, RocLab software program – free download from the Rocscience website www.rocscience.com.